Influence of group-velocity-dispersion effects on the propagation of femtosecond laser pulses in air at different pressures

Su-Yu Li, Fu-Ming Guo, Yang Song, An-Min Chen,[*] Yu-Jun Yang,[†] and Ming-Xing Jin[‡]
Institute of Atomic and Molecular Physics, Jilin University, Changchun 130012, China
(Received 28 September 2013; published 10 February 2014)

The influence of group-velocity-dispersion (GVD) effects on the propagation of femtosecond laser pulses in air at different pressures is investigated by numerically solving the extended nonlinear Schrödinger equation. It is observed that GVD has a great influence on the collapse distance L_c of the self-focusing short laser pulses when the pressure is relatively high (e.g., 10 atm), in which case the semiempirical formula describing the collapse distance of self-focusing laser pulse [Dawes and Marburger, Phys. Rev. **179**, 862 (1969)] is no longer applicable, while GVD has little influence on the self-focusing process of longer laser pulses. Through the results of numerical simulations as well as analytical analysis, we find that the initial duration of the laser pulse is the main factor that determines the GVD effect on the propagation and the increase of the pressure and pulse compression during the propagation enhance this effect. The spectral data show that GVD also influences the spectrum broadening in high-pressure cases.

DOI: 10.1103/PhysRevA.89.023809 PACS number(s): 42.65.Jx, 42.65.Re, 52.35.Mw, 42.65.Tg

I. INTRODUCTION

Since the first experimental observations of filament propagation in air in 1995 [1], femtosecond laser pulse propagation has attracted a great deal of interest in recent years due to its potential and promising applications including the generation of few-cycle optical pulses and high-order-harmonic generation [2–4], terahertz radiation [5,6], light detection and ranging (LIDAR) [7,8], rainmaking [9,10], and lightning protection [11–13]. In parallel with experimental progress, the theory and simulation of laser filamentation have gained great success.

Whether in the classical model (i.e., filamentation is described as a dynamic balance between Kerr self-focusing and plasma defocusing) [1,14,15] or in the higher-order Kerr model (i.e., filamentation is described as a dynamic balance between Kerr self-focusing and defocusing by the higher-order Kerr effect), which has drawn much attention in recent years [16,17], the laser filamentation is attributed to the nonlinear interaction. In this case, little attention has been paid to the linear effects, the group-velocity-dispersion (GVD) effect included, and in a review by Couairon and Mysyrowicz, they pointed out that "in gases, GVD is too small to play a significant role in the arrest of collapse" [15], which has been widely accepted. Indeed, most of the research on the influence of GVD on the laser propagation mainly focuses on condensed matter, such as fused-silica [18], BK7 glass [19], and optical fiber [20]; only a few works are devoted to the high-pressure gases ($p > 100$ atm, the density of the gas is close to that of condensed matter) [21] and a few of them concentrate on the case in which the pressure is relatively high (1 atm $\leqslant p \leqslant$ 10 atm).

In several previous work, it was found that GVD can cause the pulse splitting in time, which is able to arrest the pulse collapse [19,22–27]. However, this mechanism is relevant for pulses having enough power, as the critical power for collapse in dispersive media increases with dispersion [24]. For pulses with powers largely exceeding the critical power for self-focusing, the asymmetric pulse splitting promoted by plasma formation is an even more efficient mechanism than GVD in arresting the collapse and it leads to multiple splitting beyond the nonlinear focus [28–30]. For this reason, pulse splitting is not systematically induced by GVD [18]. In this paper, we focus on air at different pressures, making dispersion potentially relevant, and the powers of incident laser pulses chosen are several times larger than the critical one. The pulse splitting scenario in that case will be studied, thus investigating the GVD effect on propagation more thoroughly.

As the pressure of the gas increases, all the nonlinear indices in the nonlinear terms, say, the Kerr effect, plasma defocusing, and multiphoton ionization, scale with the pressure and the corresponding balance between them should be unaffected by pressure changes; however, the indices in the linear effects, especially GVD, also increase with the pressure at the same time, which may bring about changes during self-focusing as well as the subsequent propagation. Therefore, the influence of pressure should be taken into consideration in the theoretical research so as to describe the propagation process more accurately. In fact, in theoretical and experimental investigations as well as practical applications, the pressure we often deal with is not a standard atmospheric pressure. For instance, for lightning protection, LIDAR, and rainmaking, the pressure evolves from 1 to 0.2 atm at an attitude of 11 km [31,32]; in regard to the high-order-harmonic generation, the pressure is often chosen as 0.1 atm [33,34]; Kartashov *et al.* generated white light over three octaves by a femtosecond filament at 3.9 μm in argon by changing the pressure [35]; Popmintchev *et al.* increase the pressure to 80 atm, theoretically generating a pulse as short as 2.5 as [36].

Based on the above considerations, the propagation of a femtosecond laser pulse in air at different pressures is numerically simulated in this paper. At relatively high input power [$P_{\rm in}(p) = 8P_{\rm cr}(p)$], the influence of GVD on the process of propagation, particularly the pulse collapse, is investigated with different pressure (1 atm $\leqslant p \leqslant$ 10 atm) and pulse duration.

[*]amchen@jlu.edu.cn
[†]yangyj@jlu.edu.cn
[‡]mxjin@mail.jlu.edu.cn

The paper is organized as follows. In Sec. II, we recall the nonlinear Schrödinger equation (NLSE) describing the femtosecond pulse propagation in air at different pressures. In Sec. III, by freezing the ratio of input pulse power to the critical one of self-focusing, we investigate the influence of GVD on a femtosecond laser pulse in air with the pressure varying between 1 and 10 atm and explore the factors that determine this influence. Finally, the main conclusion is summarized in Sec. IV.

II. THEORETICAL METHOD

The propagation of a laser pulse in air can be informed from the evolution of the scalar electric field envelope $E(r,z,t)$ (where $I = |E|^2$ is the pulse intensity given in units of W/m^2) along the propagation direction z, which is governed by the NLSE in the reference frame moving at the group velocity:

$$\frac{\partial E}{\partial z} = \frac{i}{2k_0}\left(\frac{\partial^2}{\partial r^2} + \frac{1}{r}\frac{\partial}{\partial r}\right)E - \frac{ik''}{2}\frac{\partial^2 E}{\partial \tau^2} - \frac{\sigma}{2}(1+i\omega_0\tau_c)n_e E + ik_0 n_2|E|^2E - \frac{\beta_K|E|^{2K-2}E}{2}, \quad (1)$$

where $\tau = t - z/v_g$ refers to the retarded time for a pulse traveling at the group velocity $v_g = \partial\omega/\partial k|_{\omega_0}$; $k_0 = 2\pi/\lambda_0$ and $\omega_0 = 2\pi c/\lambda_0$ are the wave number and the angular frequency of the carrier wave, respectively. Here the first term accounts for the transverse diffraction and the remaining terms refer to the normal GVD with the coefficient $k'' = \partial^2 k/\partial\omega^2|_{\omega_0}$, plasma absorption (real part) and plasma defocusing (imaginary part) with the inverse bremsstrahlung cross section σ and electron collision time τ_c, and the Kerr effect of air with the nonlinear index of refraction n_2 (i.e., Kerr index). The last term describes multiphoton absorption with the coefficient $\beta_K = K\hbar\omega_0 n_{air}\sigma_K$, where σ_K accounts for the multiphoton ionization coefficient and n_{air} is number density of air. Here $K = \text{mod}(U/\hbar\omega_0 + 1)$ is the minimum number of photons needed in the multiphoton ionization process and with $U = 11$eV is the characteristic ionization energy of air.

The evolution of electron density n_e can be calculated as [37]

$$\frac{\partial n_e}{\partial \tau} = \frac{n_e}{U}\sigma|E|^2 + \frac{\beta_K|E|^{2K}}{K\hbar\omega_0} - a n_e^2. \quad (2)$$

The first term on the right-hand side of Eq. (2) accounts for the avalanche ionization, the second term refers to the multiphoton ionization, and the last term describes the electron recombination with coefficient $a = 5.0\times10^{-13}$ m^3/s.

Most of the parameters in Eqs. (1) and (2) are related to the pressure: $n_2(p) = n_2(p_0)\tilde{p}$, $\tau_c(p) = \tau_c(p_0)/\tilde{p}$, $\sigma(p) = \sigma(p_0)\frac{\tilde{p}[1+\omega_0^2\tau_0^2(p_0)]}{\tilde{p}^2+\omega_0^2\tau_0^2(p_0)}$, $k''(p) = k''(p_0)\tilde{p}$, $n_{air}(p) = n_{air}(p_0)\tilde{p}$, and $\beta_K(p) = \beta_K(p_0)\tilde{p}$. Here we set $\tilde{p} = p/p_0$, where p_0 denotes a standard atmospheric pressure and p stands for the practical pressure of gas.

Self-focusing is one of the most fundamental and important phenomena in the process of the propagation of intense laser pulse and for the Gaussian pulse, the propagation length of the self-focusing beam until collapse L_c (here we call it collapse distance) can be well described by a semiempirical formula [38,39]

$$L_c = 0.367k_0w_0^2\Big/\{[(P_{in}/P_c)^{1/2} - 0.852]^2 - 0.0219\}^{1/2}, \quad (3)$$

where $P_{cr} = 3.77\lambda_0^2/8\pi n_0 n_2$ is the critical power of self-focusing [39], P_{in} denotes the power of incident laser pulse, and w_0 accounts for the initial beam radius. In the paper, we select a Gaussian pulse whose envelope can be written as $E(r,t) = E_0\exp(-r^2/w_0^2)\exp(-t^2/\tau_0^2)$ and the initial beam radius and wavelength are selected as $w_0 = 1.2$ mm and $\lambda_0 = 775$ nm, respectively. In a standard atmospheric pressure, the values of the nonlinear refraction index, GVD coefficient, critical power of self-focusing, multiphoton absorption coefficient, electron collision time, and inverse bremsstrahlung cross section are $n_2 = 3.2\times10^{-23}$ m^2/W, $k'' = 2\times10^{29}$ s^2/m, $P_c = 2.815$ GW, $\beta_7 = 6.5\times10^{-104}$ m^2/W^9, $\tau_c = 3.5\times10^{-13}$ s, and $\sigma = 5.1\times10^{-24}$ m^2, respectively (the values of parameters β_7, τ_c, and U are from Ref. [40]). In view of the fact that $n_2(p) = n_2(p_0)\tilde{p}$ and $P_{cr} = 3.77\lambda_0^2/8\pi n_0 n_2$, the critical power of self-focusing is inversely proportional to the pressure, i.e., $P_{cr}(p) = P_{cr}(p_0)/\tilde{p}$. It can be clearly seen from Eq. (3) that in the case that $P_{in}(p)/P_{cr}(p)$ and w_0 are fixed, the collapse distance L_c is independent of pressure and pulse duration. Therefore, for the purpose of facilitating the research, the power of the incident laser pulses is set as $P_{in}(p) = 8P_{cr}(p)$ throughout this paper.

III. RESULTS AND DISCUSSION

Figure 1 shows the change of the on-axis intensity [Figs. 1(a) and 1(a′)], electron density [Figs. 1(b) and 1(b′)], and beam radius [Figs. 1(c) and 1(c′)] of the 50-fs laser pulse with the propagation distance z at 1 atm (solid black

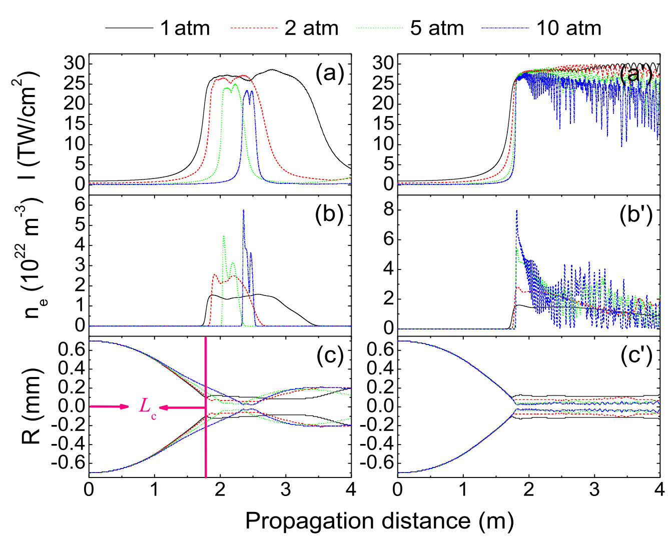

FIG. 1. (Color online) Variation of the (a) and (a′) on-axis intensity, (b) and (b′) electron density, and (c) and (c′) beam radius of the laser pulse with the propagation distance z at 1 atm (solid black curves), 2 atm (dashed red curves), 5 atm (dotted green curves), and 10 atm (dash-dotted blue curves) in the cases that GVD is (a)–(c) considered and (a′)–(c′) neglected. The duration of the incident laser pulse is 50 fs.

curves), 2 atm (dashed red curves), 5 atm (dotted green curves), and 10 atm (dash-dotted blue curves) in the cases in which GVD is considered [Figs. 1(a)–1(c)] and neglected [Figs. 1(a′)–1(c′)], respectively. It can be seen from the figure that, as the pressure increases, the clamping intensity at the beginning of the filament nearly remains unchanged, staying around 2.5×10^{17} W/m^2, the on-axis electron density is proportional to the pressure, and the beam radius becomes smaller; these observations are in agreement with the phenomena observed in low-pressure cases [31,41] and exist whether the GVD is considered or neglected. As for the cause of these phenomena, in Ref. [31] Champeaux and Bergé discussed them on the basis of simple analytical arguments. It should be noted that there is a difference between this work and that in Ref. [31]: The input power P_{in} at ground level is a fixed value [31], while the input power P_{in} used here changes with the pressure accordingly, but its ratio to $P_{\text{cr}}(p)$ is fixed. This accounts for the difference: The intensity at the beginning of the filament exhibits a tendency to decrease with an increase of the pressure, which we will analyze later.

In addition, a more obvious difference is that, in the case in which GVD is considered, the collapse distance of the self-focusing pulse L_c [in our work, the collapse distance is defined as the distance between the light source and the position where the laser beam has the smallest radius; L_c in Fig. 1(c) represents the collapse distance of a 50-fs laser pulse in air at 1 atm] increases with an increase in pressure, as shown in Fig. 1(c). In contrast, in the case in which GVD is neglected, L_c does not change with pressure, as shown in Fig. 1(c′). However, we can see from Eq. (3) that once $P_{\text{in}}(p)/P_{\text{cr}}(p)$ and w_0 are fixed, L_c is independent of the pressure. This semiempirical formula cannot thus be used to describe pulse self-focusing with dispersion at high pressures, while it is still suitable for cases in which GVD is neglected.

Starting with the propagation equation (1), we can analyze the above phenomena. At normal and low pressures, the indices in the linear terms (e.g., GVD coefficient k'') are small; during the propagation of the laser pulse in gas, the nonlinear effects are much stronger than the linear ones due to the high intensity adopted. For this reason, much attention has been paid to the action of the nonlinear effects and the role of linear effects is not considered. However, as regards the relatively high pressure, although all the indices in nonlinear terms scale with the pressure resulting in the corresponding balance between the nonlinear effects, the indices in the linear effects increase at the same time, thus affecting the self-focusing process of the laser beam, in particular, the process before the collapse. It is just the case for GVD and at the initial position (i.e., $z_0 = 0$ m) the polarization $P_{\text{GVD}}(r,z_0,t) = \frac{k''}{2}\frac{\partial^2 E(r,z_0,t)}{\partial \tau^2}$ induced by GVD in the frequency domain is given as

$$P_{\text{GVD}}(r,z_0,\omega) = \tilde{F}[P_{\text{GVD}}(r,z_0,t)] = \frac{k''}{2}\omega^2 E(r,z_0,\omega)$$
$$= k'' E_0 \exp\left(-r^2/w_0^2\right)\frac{\omega^2\tau_0}{2\sqrt{2}}\exp\left(-\omega^2\tau_0^2/4\right), \quad (4)$$

where $\tilde{F}$ denotes the Fourier transformation and the frequency ω refers to the difference between the spectrum and central frequency of the incident laser pulse. It should be noted here that Eq. (1) is often solved in the frequency domain; more details about the numerical methods can be found in Ref. [42]. Here we set $P_{\text{GVD}}(r,z_0,\omega) = k'' E_0 H(\omega) G(r)$ with $H(\omega) = \frac{\omega^2\tau_0}{2\sqrt{2}}\exp(-\omega^2\tau_0^2/4)$ and $G(r) = \exp(-r^2/w_0^2)$. In the case shown in Fig. 1, the pulses adopted are 50 fs, the expressions of $H(\omega)$ are the same, and thus the amplitude of $P_{\text{GVD}}(r,z_0,\omega)$ is determined by the product of k'' and E_0, where $k''(p) = k''(p_0)\tilde{p}$, $E_0(p) = \sqrt{2P_{\text{in}}(p)/\pi w_0^2} = \sqrt{2P_{\text{in}}(p_0)/\pi w_0^2 \tilde{p}} = E_0(p_0)/\sqrt{\tilde{p}}$, and $k''(p)E_0(p) = k''(p_0)E_0(p_0)\sqrt{\tilde{p}}$. Therefore, along with the increase in pressure, the amplitude of $P_{\text{GVD}}(r,z_0,\omega)$ increases and the defocusing by GVD increases, thus counteracting the Kerr self-focusing to a certain degree and increasing L_c. Furthermore, after the collapse, GVD will act in combination with the plasma effect to enhance the defocusing effect and thereby arrest the increase of the intensity. As a result, we see in Fig. 1(a) that the clamping intensity shows a tendency to decrease as the pressure increases.

It can be seen from the expression of $P_{\text{GVD}}(r,z_0,\omega)$ that the influence of GVD on the propagation process is also related to $H(\omega)$, which depends on the duration of the laser pulse τ_0. Therefore, we calculate the propagation of four laser pulses whose respective durations are 50, 70, 110, and 330 fs in air at 10 atm so as to investigate the relation between pulse durations and the influence of GVD on the propagation, as shown in Fig. 2. We can see from the figure that the collapse distances L_c of the four pulses are identical to each other in the case in which GVD is neglected [see Fig. 2(c′)], while L_c decreases as the pulse duration increases in the case in which GVD is considered [see Fig. 2(c)]. As a result, in the case of 330 fs, L_c is almost identical to the collapse distance when GVD is

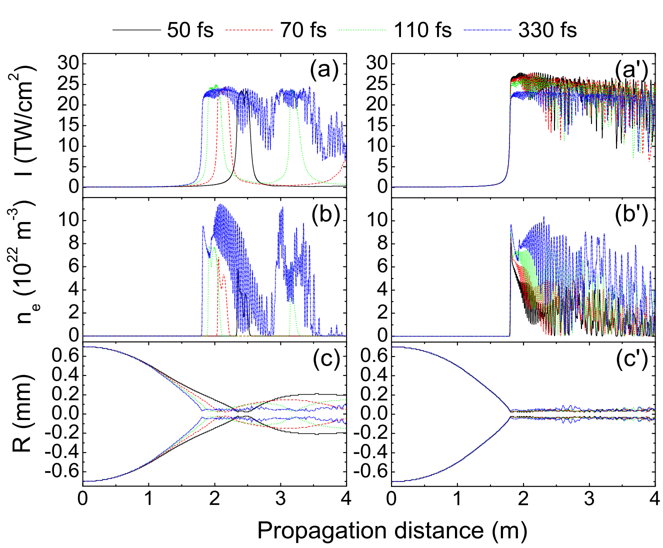

FIG. 2. (Color online) Variation of the (a) and (a′) on-axis intensity, (b) and (b′) electron density, and (c) and (c′) beam radius of the laser pulses with the propagation distance z at 10 atm in the cases that GVD is (a)–(c) considered and (a′)–(c′) neglected. The durations of the incident laser pulses are 50 fs (solid black curves), 70 fs (dashed red curves), 110 fs (dotted green curves), and 330 fs (dash-dotted blue curves), respectively.

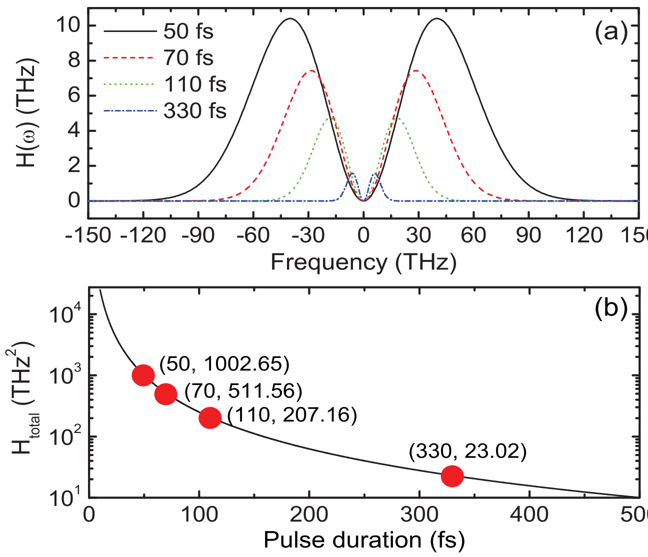

FIG. 3. (Color online) (a) Evolution of the function $H(\omega) = (\omega^2\tau_0/2\sqrt{2})\exp(-\omega^2\tau_0^2/4)$ with frequency as the initial pulse durations are 50 fs (solid black curve), 70 fs (dashed red curve), 110 fs (dotted green curve), and 330 fs (dash-dotted blue curve), respectively. (b) Evolution of H_{total} [$H_{\text{total}} = \int_{-\infty}^{+\infty} H(\omega)d\omega$] with the initial duration of the laser pulse.

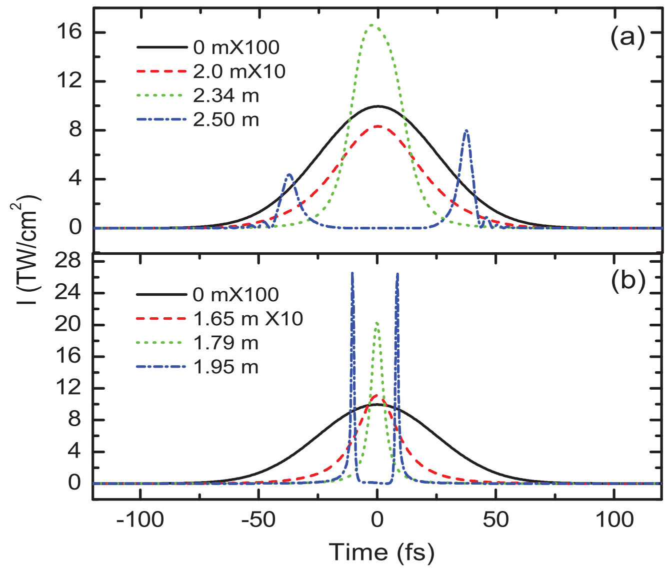

FIG. 4. (Color online) (a) Time evolution of the laser pulse with GVD considered at $z = 0$, 2.0, 2.34 (collapse distance), and 2.5 m, respectively. (b) Time evolution of the laser pulse with GVD neglected at $z = 0$, 1.65, 1.79 (collapse distance), and 1.95 m, respectively. The initial pulse duration and pressure are chosen as 50 fs and 10 atm, respectively, corresponding to the 50-fs cases shown in Fig. 2.

neglected [see the dash-dotted blue curves in Figs. 2(c) and 2(c′)].

As for the phenomena described above, they can still be explained by analyzing the GVD term. We present in Fig. 3(a) the change of the function $H(\omega) = \frac{\omega^2\tau_0}{2\sqrt{2}}\exp(-\omega^2\tau_0^2/4)$ with frequency for initial pulse durations of 50, 70, 110, and 330 fs, respectively. As stated previously, $\frac{\tau_0}{\sqrt{2}}\exp(-\omega^2\tau_0^2/4)$ in $H(\omega)$ is actually the Fourier transformation of $E(t) = \exp(-t^2/\tau_0^2)$, which shows the frequency characteristic of the laser pulse, and we can see from the figure that the spectral range is inversely associated with the duration of the laser pulse. In practice, the strength of the GVD effect is determined by the total polarization, which is obtained by integrating $P_{\text{GVD}}(r,z_0,\omega)$ in the frequency domain (we borrow the definition of polarization in the field of electromagnetism, which is here integrated in space). It is obvious that the total polarization is in proportion to H_{total}, which is the integral of $H(\omega)$ in the whole frequency domain [i.e., $H_{\text{total}} = \int_{-\infty}^{+\infty} H(\omega)d\omega$]. From the closed red circles in Fig. 3(b), we see that the values of H_{total} are 1002.65, 511.56, 207.16, and 23.02 THz^2 for the 50-, 70-, 110-, and 330-fs pulses and the value of H_{total} in the case of 330 fs is about 43 times smaller than that in the case of 50 fs. As a result, even at high pressure ($p = 10$ atm), the total polarization is very small and the influence of GVD on the self-focusing process is tiny for the longer pulse [see the dash-dotted blue curves in Figs. 2(c) and 2(c′)]. As for the case in Fig. 2, the pressure p is set as 10 atm, the values of $k''(p)$ and $E_0(p)$ are fixed, shorter pulse duration leads to larger value of H_{total}, and thereby the defocusing by GVD for shorter laser pulses becomes stronger than that for longer laser pulses at high pressures, making L_c of shorter pulses longer. Thus, we can infer that even if the pressure is low, GVD plays a great role in the pulse collapse for shorter pulses. Furthermore, the value of k'' increases sharply with the decrease of the wavelength of the laser pulse. As a result, GVD also plays a significant role in the propagation of a laser pulse whose wavelength ranges from extreme ultraviolet to soft x ray. For this reason, in the research of high-order-harmonic generation that considers the propagation effect, GVD should not be neglected.

It is obvious that the expression of $P_{\text{GVD}}(r,z,\omega)$ will be changed during the propagation. The pulse duration can indeed be compressed, as shown in Fig. 4(a), and at the same time the corresponding spectrum will be broadened due to the self-phase modulation [43]. We learn from Fig. 3 that as the spectrum becomes wider, the integral of $H(\omega)$ will become larger, thus enhancing the strength of the GVD effect. For this reason, we can say that what mainly determines the GVD effect on the laser propagation is the initial duration of the laser pulse and the spectrum broadening during the propagation only enhances the effect. In addition, it can be seen from Figs. 4(a) and 4(b) that the pulses are compressed during the propagation process whether the GVD is considered or not and at the collapse distance the laser pulses do not experience splitting in time in both cases (dotted green curves), while after the collapse distance, the pulses split in time (dash-dotted blue curves). Moreover, the on-axis electron density increases tremendously around the collapse distance [see the solid black curves in Figs. 2(b) and 2(b′)], which means that plasma generation plays a key role in arresting the pulse collapse. This is in agreement with the conclusion in Refs. [28–30], i.e., for pulses with powers largely exceeding the critical power for self-focusing, the asymmetric pulse splitting promoted by plasma formation is an even more efficient mechanism than GVD in arresting the collapse beyond the nonlinear focus and the conclusion that pulse splitting is not systematically induced by GVD [18] is confirmed.

As shown in Figs. 2(b) and 2(b′), the on-axis electron density increases with an increase of pulse duration. This phenomenon is attributed to the fact that as the pulse duration increases, the interaction time with air becomes longer and more air is ionized. As for the case in which GVD is considered, as the pulse duration is longer, the corresponding on-axis electron density becomes larger [see Fig. 2(b)], the plasma defocusing becomes stronger, and GVD becomes weaker. As a result, the overall defocusing effect changes a little and the dynamic balance between it and Kerr self-focusing does not change, thus leading to the fact that the clamping intensity does not vary with the pulse duration, as shown in Fig. 2(a). However, only the plasma effect plays the role of defocusing in the case in which GVD is neglected. The plasma density increases with an increase of pulse duration [see Fig. 2(b′)] and its defocusing effect becomes stronger, resulting in a tendency to decrease the clamping intensity, as shown in Fig. 2(a′).

It should be noted that in the case in which GVD is neglected, the plasma range does not change much when the pressure and pulse duration are changed and is much longer compared with the case in which GVD is considered, as shown in Figs. 1(b), 1(b′), 2(b), and 2(b′). Skupin *et al.* reported that omitting GVD prevents the different time slices of the pulse from exchanging power (energy) and thereby from shortening the plasma range [44]. Here, combining the behaviors of collapse distance L_c, on-axis intensity, electron density, and beam radius shown in Fig. 1 with those shown in Fig. 2, the conclusion in Ref. [45] that GVD may have some importance not only during the self-channeling regime, but also after plasma generation over meter-range distances can be verified and extended to the high-pressure cases.

As is known, the introduction of temporal chirp can not only increase the spectral range of the laser pulse but also change the pulse duration. Consequently, after introducing the chirp, even if the incident laser pulse is a longer one, the collapse distance will be affected. The electric field can be expressed as Eq. (4) with the chirp being introduced [41,46]:

$$E(r,t)=E_0 \exp\left(-r^2/w_0^2\right) \exp\left(-t^2/\tau_0^2\right) \exp\left(-iCt^2/\tau_0^2\right), \tag{5}$$

where C denotes the chirp of the incident pulse that is linked to the minimum pulse duration $\tau_p^{\min} = \tau_p/\sqrt{1+C^2}$ and the second order derivative $\phi^{(2)} = C\tau_p^2/2(1+C^2)$ [41].

Figure 5 details the propagation of a 330-fs laser pulse with a temporal chirp of $\phi^{(2)} = -8.25 \times 10^2$ fs^2 ($\tau_p^{\min}$= 5 fs) in air at 10 atm as GVD is considered [Figs. 5(a)–5(c)] and neglected [Figs. 5(a′)–5(c′)] and compares it with the case without any chirp. From the figure we can see that as GVD is considered, compared with the collapse distance L_c of the pulse without any chirp, that of the pulse with a temporal chirp will be larger, as shown in Fig. 5(c). In contrast, as GVD is neglected, even if the laser pulse is chirped, the collapse distance of it is identical to that of the pulse without any chirp. Furthermore, the evolutions of on-axis intensity, electron density, and beam radius in the two cases are completely identical to each other, as shown in Figs. 5(a)–5(c′). This phenomenon can be well

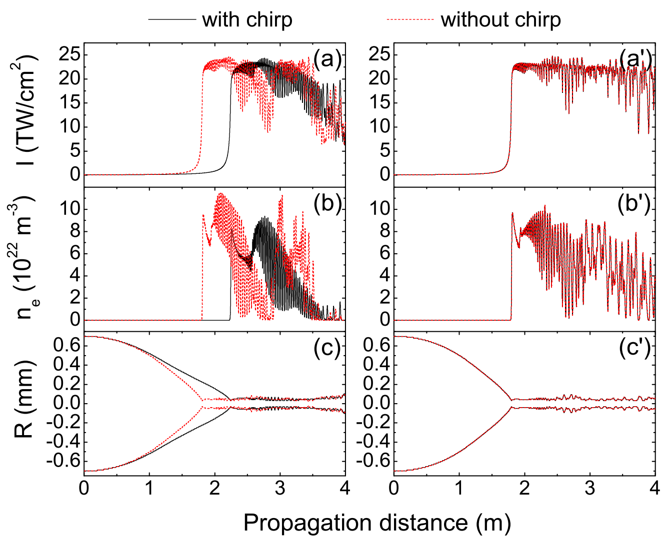

FIG. 5. (Color online) Variation of the (a) and (a′) on-axis intensity, (b) and (b′) electron density, and (c) and (c′) beam radius of the laser pulses with the propagation distance z at 10 atm as GVD is (a)–(c) considered and (a′)–(c′) neglected. The solid black curves denote the case with a chirp of $\phi^{(2)} = -8.25 \times 10^2$ fs^2 (input pulse duration of 330 fs) and the dashed red curves denote the case without any chirp.

explained by Eq. (13), i.e.,

$$T(z) = T_0\sqrt{\left(1+\frac{2k''Cz}{t_0^2}\right)^2 + \left(\frac{2k''z}{t_0^2}\right)^2},$$

where $T(z)$ is the evolution of pulse duration along the propagation direction z, in Ref. [47], and once GVD is neglected, whether the chirp is introduced or not, the evolution of the pulse duration shows no difference in the two cases. This result further confirms the dominant role that GVD plays in affecting the propagation process, especially the pulse collapse.

Figure 6(a) shows the change of L_c with the pressure for a pulse duration of 50 fs and Fig. 6(b) shows the change of L_c with the pulse duration for a pressure of 10 atm. It can be seen from the figure that in the case in which $P_{in}(p)/P_{cr}(p)$ and w_0 are fixed, the collapse distance L_c is independent of the pressure and pulse duration when GVD is neglected [see the closed red circles in Figs. 6(a) and 6(b)]. In contrast, when GVD is considered, along with an increase in pressure and a decrease in pulse duration, L_c will become larger [see the closed black squares in Figs. 6(a) and 6(b)]. For instance, at 10 atm, the collapse distance for a 330-fs laser pulse is $L_c = 1.79$ m, while that of the 50-fs pulse is $L_c = 2.34$ m, which is 30% larger than the former. In addition, the behavior of the closed black squares in Fig. 6(b) is somewhat similar to that of the solid black curves in Fig. 3(b); however, their asymptotic behaviors with respect to the time axes are different due to the pulse compression during the propagation before the pulse collapse. The above facts combined with the former analysis and discussion lead to the following conclusions: The initial duration of the laser pulse is the main factor that determines the GVD effect on the propagation process, especially the pulse collapse, and the

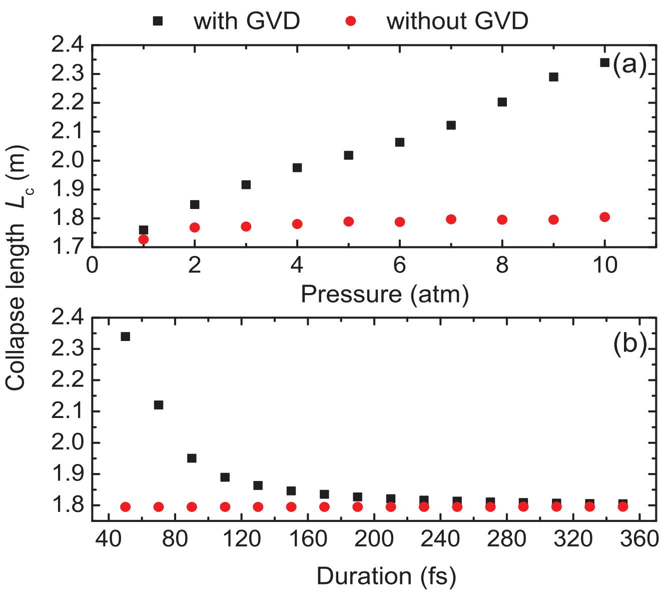

FIG. 6. (Color online) (a) Change of L_c with pressure for a pulse duration of 50 fs. (b) Change of L_c with pulse duration for a pressure of 10 atm.

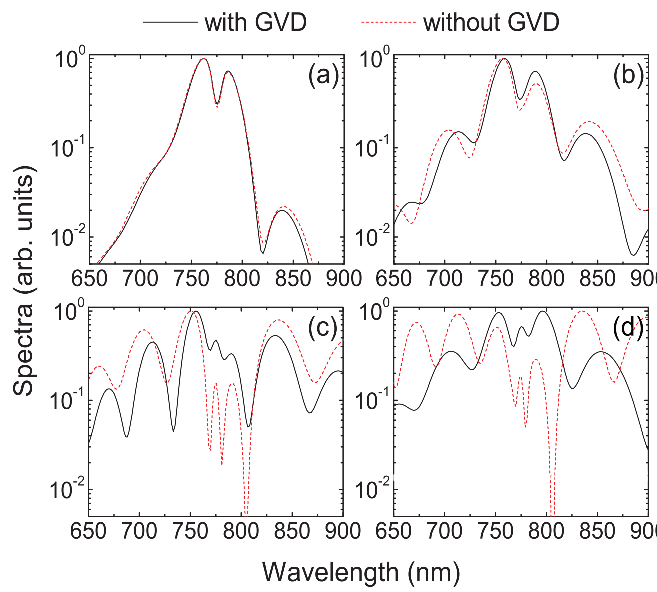

FIG. 7. (Color online) Spectra of the laser pulses whose durations are 90 fs at the propagation distance $z = 2.0$ m at (a) 1 atm, (b) 2 atm (c) 5 atm, and (d) 10 atm with the GVD effect considered (solid black curves) and neglected (dashed red curves), respectively.

increases in gaseous pressure and pulse compression during the propagation enhance this effect. Only in the case of shorter pulses can this effect be obvious. Therefore, Eq. (3) is applicable for laser pulses whose duration is not too short at normal and low pressures as well as for the longer pulses at high pressures. However, there still exists a minor difference between the L_c of the cases with GVD being considered and neglected and the influence of GVD on the L_c of longer pulse can be observed at higher pressures, which is still not apparent though. In Refs. [48–50], a universal map for wave collapse depending on the normalized GVD coefficient versus power ratio was created, which can resoundingly show under what initial condition the collapse can occur and the boundaries of dispersion-dominated and self-focusing-dominated regimes. If we take the pressure-dependent GVD coefficient k'' into consideration, a more universal map can be made. However, this kind of map fails to predict the exact value of the collapse distance. For this reason, to make the semiempirical self-focusing formula universal for more cases, the influence of pulse duration and pressure as well as pulse compression during the propagation before the pulse collapse should be considered to modify it, which needs further research.

As the pressure increases, the spectrum broadening degree of the laser pulse is bound to be affected due to the enhancement of the GVD effect. In Fig. 7, we present the spectra of the 90-fs laser pulses propagating in air at 1, 2, 5, and 10 atm at $z = 2.0$ m (after the pulse collapse). It is found that at 1 atm, the spectrum obtained in the case considering GVD is identical to that obtained in the case neglecting GVD, indicating that GVD has little influence on the spectrum broadening [see Fig. 6(a)] at low pressures, which is somewhat similar to the phenomenon shown Fig. 3 in Ref. [16], though different models are adopted. As we increase the pressure gradually, the spectrum broadening degree becomes greater both in the case in which GVD is considered and that in which it is neglected [see Figs. 7(c) and 7(d)], indicating that increasing the pressure can enlarge the spectrum broadening degree of the laser pulse, which has been applied to the preparation of supercontinua and ultrashort pulses [35,36,51]. As shown in Figs. 6(b)–6(d), for the case in which GVD is neglected, the spectrum broadening degree is larger, which is caused by the difference in the collapse distances in the two cases: When GVD is neglected, the collapse distances are all located at $L_c = 1.79$ m [see the red circle in Figs. 6(a) and 6(b)]; when GVD is considered, the collapse distances get closer and closer to the propagation distance $z = 2.0$ m during the increase in pressure. This indicates that, in the case in which GVD is considered, the distance between the collapse position and $z = 2.0$ m becomes shorter as the pressure increases and the changes that spectra experience will get smaller. As a result, the spectrum broadening degree in the case in which GVD is considered is not as large as that in the case in which GVD is neglected.

Previous study suggested that in normally dispersive media, GVD will affect the self-focusing process of a laser pulse [18–20,24,50]. At ambient and low pressures in gases, the GVD coefficient is small and compared with the nonlinear effects, the GVD effect is quite weak, with a small influence on the self-focusing process, which is thus neglected. For this reason, Couairon and Mysyrowicz pointed out that, in gases, GVD is too small to play a significant role in the arrest of collapse [15]. However, when we increase the pressure of the gas, the GVD coefficient increases correspondingly, greatly affecting the collapse of the pulse during the self-focusing. In practice, for $p > 10$ atm GVD can become a significant factor in gases. As a result, we find in this paper that, at high pressure, GVD not only greatly affects the collapse distance L_c, but also influences the clamping intensity, on-axis electron density, beam radius, and even the spectrum of the laser pulse.

IV. CONCLUSION

In this paper, in the case of freezing the ratio of input pulse power to the critical one of self-focusing, we investigated the influence of GVD on the propagation of the femtosecond laser pulses in air at different pressures. Previous works suggested that GVD is too small to play a significant role in the arrest of collapse in gases, which is true for the cases at normal or low pressures. However, in the case in which the pressure is relatively high (say, 10 atm), the GVD coefficient scales with the pressure and GVD will have a great influence on the collapse distance of the self-focusing shorter laser pulses, which cannot be explained by the semiempirical self-focusing formula apparently. Through the results of numerical simulations as well as the explanation of the qualitative role of GVD given in terms of the Fourier transformation of the GVD term, it was found that the influence of GVD on the laser propagation mainly depends on the initial duration of the laser pulses and the increase of the gaseous pressure and pulse compression during the propagation enhance this effect: For the shorter pulses, GVD still has a great influence on their propagation even if the pressure is not that high. For the longer pulses, the influence of GVD on their propagation is not obvious, however, if a temporal chirp is introduced in them, GVD will also affect the propagation. Making the semiempirical formula (3) applicable when including GVD will need further research. In summary, the investigation of the influence of GVD on the laser spectra after the pulse collapse revealed that, at normal pressure, GVD influences the spectrum broadening a little, while at higher pressures, it affects the spectrum broadening greatly.

ACKNOWLEDGMENTS

This work was supported by the National Basic Research Program of China (973 Program) No. 2013CB922200, the Research Fund for the Doctoral Program of Higher Education (Grant No. 20130061110021), the National Natural Science Foundation of China (Grants No. 11034003, No. 10974069, No. 11274141, and No. 11304116), and the Project supported by the Jilin Provincial Research Foundation for Basic Research, China (Grant No. 20140101168JC).

[1] A. Braun, G. Korn, X. Liu, D. Du, J. Squier, and G. Mourou, Opt. Lett. **20**, 73 (1995).
[2] C. P. Hauri, W. Kornelis, F. W. Helbing, A. Heinrich, A. Couairon, A. Mysyrowicz, J. Biegert, and U. Keller, Appl. Phys. B **79**, 673 (2004).
[3] Y. Tamaki, J. Itatani, Y. Nagata, M. Obara, and K. Midorikawa, Phys. Rev. Lett. **82**, 1422 (1999).
[4] V. Tosa, E. Takahashi, Y. Nabekawa, and K. Midorikawa, Phys. Rev. A **67**, 063817 (2003).
[5] C. D'Amico, A. Houard, M. Franco, B. Prade, A. Mysyrowicz, A. Couairon, and V. T. Tikhonchuk, Phys. Rev. Lett. **98**, 235002 (2007).
[6] S. Tzortzakis, G. Méchain, G. Patalano, Y.-B. André, B. Prade, M. Franco, A. Mysyrowicz, J.-M. Munier, M. Gheudin, G. Beaudin, and P. Encrenaz, Opt. Lett. **27**, 1944 (2002).
[7] J. Kasparian, M. Rodriguez, G. Mjean, J. Yu, E. Salmon, H. Wille, R. Bourayou, S. Frey, Y.-B. André, A. Mysyrowicz, R. Sauerbrey, J. P. Wolf, and L. Wöste, Science **301**, 61 (2003).
[8] R. Bourayou, G. Méjean, J. Kasparian, M. Rodriguez, E. Salmon, J. Yu, H. Lehmann, B. Stecklum, U. Laux, J. Eislöffel, A. Scholz, A. P. Hatzes, R. Sauerbrey, L. Wöste, and J.-P. Wolf, J. Opt. Soc. Am. B **22**, 369 (2005).
[9] P. Rohwetter, J. Kasparian, K. Stelmaszczyk, Z. Q. Hao, S. Henin, N. Lascoux, W. M. Nakaema, Y. Petit, M. M. Queisser, R. Salam, E. Salmon, L. Wöste, and J.-P. Wolf, Nat. Photon. **4**, 451 (2010).
[10] J. J. Ju, J. S. Liu, C. Wang, H. Y. Sun, W. T. Wang, X. C. Ge, C. Li, S. L. Chin, R. X. Li, and Z. Z. Xu, Opt. Lett. **37**, 1214 (2012).
[11] S. Tzortzakis, B. Prade, M. Franco, A. Mysyrowicz, S. Hüller, and P. Mora, Phys. Rev. E **64**, 057401 (2001).
[12] R. Ackermann, K. Stelmaszczyk, P. Rohwetter, G. Méjean, E. Salmon, J. Yu, J. Kasparian, G. Méchain, V. Bergmann, S. Schaper, B. Weise, T. Kumm, K. Rethmeier, W. Kalkner, J.-P. Wolf, and L. Wöste, Appl. Phys. Lett. **85**, 5781 (2004).
[13] J.-C. Diels, R. Bernstein, K. E. Stahlkopf, and X. M. Zhao, Sci. Am. **277**(2), 50 (1997).
[14] L. Bergé, S. Skupin, R. Nuter, J. Kasparian, and J.-P. Wolf, Rep. Prog. Phys. **70**, 1633 (2007).
[15] A. Couairon and A. Mysyrowicz, Phys. Rep. **441**, 47 (2007).
[16] P. Béjot, J. Kasparian, S. Henin, V. Loriot, T. Vieillard, E. Hertz, O. Faucher, B. Lavorel, and J.-P. Wolf, Phys. Rev. Lett. **104**, 103903 (2010).
[17] W. Ettoumi, P. Béjot, Y. Petit, V. Loriot, E. Hertz, O. Faucher, B. Lavorel, J. Kasparian, and J.-P. Wolf, Phys. Rev. A **82**, 033826 (2010).
[18] J. K. Ranka and A. L. Gaeta, Opt. Lett. **23**, 534 (1998).
[19] J. K. Ranka, R. W. Schirmer, and A. L. Gaeta, Phys. Rev. Lett. **77**, 3783 (1996).
[20] G. P. Agrawal, *Nonlinear Fiber Optics*, 4th ed. (Academic, Dan Diego, 2007), Chap. 3.
[21] M. Mlejnek, E. M. Wright, and J. V. Moloney, Phys. Rev. E **58**, 4903 (1998).
[22] L. Bergé and J. J. Rasmussen, Phys. Plasmas **3**, 824 (1996).
[23] L. Bergé, E. A. Kuznetsov, and J. J. Rasmussen, Phys. Rev. E **53**, R1340 (1996).
[24] G. Fibich, V. M. Malkin, and G. C. Papanicolaou, Phys. Rev. A **52**, 4218 (1995).
[25] L. Bergé, S. Champeaux, E. A. Kuznetsov, E. G. Shapiro, and S. K. Turitsyn, J. Opt. Soc. Am. B **13**, 1879 (1996).
[26] K. Germaschewski, R. Grauer, L. Bergé, V. K. Mezentsev, and J. J. Rasmussen, Physica D **151**, 175 (2001).
[27] L. Bergé, K. Germaschewski, R. Grauer, and J. J. Rasmussen, Phys. Rev. Lett. **89**, 153902 (2002).
[28] S. N. Vlasov, L. V. Piskunova, and V. I. Talanov, Sov. Phys. JETP **68**, 1125 (1989).

[29] N. E. Kosmatov, V. F. Shvets, and V. E. Zakharov, Physica D **52**, 16 (1991).
[30] A. Couairon, E. Gaižauskas, D. Faccio, A. Dubietis, and P. Di Trapani, Phys. Rev. E **73**, 016608 (2006).
[31] S. Champeaux and L. Bergé, Opt. Lett. **31**, 1301 (2006).
[32] P. Béjot *et al.*, Appl. Phys. Lett. **90**, 151106 (2007).
[33] H. C. Du and B. T. Hu, Phys. Rev. A **84**, 023817 (2011).
[34] P. F. Lan, P. X. Lu, Q. G. Li, F. Li, W. Y. Hong, and Q. B. Zhang, Phys. Rev. A **79**, 043413 (2009).
[35] D. Kartashov, S. Ališauskas, A. Pugžlys, A. Voronin, A. Zheltikov, M. Petrarca, P. Béjot, J. Kasparian, J.-P. Wolf, and A. Baltuška, Opt. Lett. **37**, 3456 (2012).
[36] T. Popmintchev *et al.*, Science **336**, 1287 (2012).
[37] E. Yablonovitch and N. Bloembergen, Phys. Rev. Lett. **29**, 907 (1972).
[38] E. L. Dawes and J. H. Marburger, Phys. Rev. **179**, 862 (1969).
[39] J. H. Marburger, Prog. Quantum Electron. **4**, 35 (1975).
[40] M. Mlejenk, E. M. Wright, and J. Moloney, Opt. Lett. **23**, 382 (1998).
[41] A. Couairon, M. Franco, G. Mchain, T. Olivier, B. Prade, and A. Mysyrowicz, Opt. Commun. **259**, 265 (2006).
[42] A. Couairon, E. Brambilla, T. Corti, D. Majus, O. d. J. Ramírez-Góngora, and M. Kolesik, Eur. Phys. J. Spec. Top. **199**, 5 (2011).
[43] A. Couairon and L. Bergé, Phys. Rev. Lett. **88**, 135003 (2002).
[44] S. Skupin, R. Nuter, and L. Bergé, Phys. Rev. A **74**, 043813 (2006).
[45] S. Champeaux and L. Bergé, Phys. Rev. E **71**, 046604 (2005).
[46] R. Nuter, S. Skupin, and L. Bergé, Opt. Lett. **30**, 917 (2005).
[47] R. Nuter and L. Bergé, J. Opt. Soc. Am. B **23**, 874 (2006).
[48] P. Chernev and V. Petrov, Opt. Lett. **17**, 172 (1992).
[49] S. Skupin and L. Bergé, Physica D **220**, 14 (2006).
[50] G. G. Luther, J. V. Moloney, and A. C. Newell, Opt. Lett. **19**, 862 (1994).
[51] L. Bergé, J. Rolle, and C. Köhler, Phys. Rev. A **88**, 023816 (2013).